

Physical Working Principles of Medical Radar

Øyvind Aardal, *Student member, IEEE*, Yoann Paichard, Sverre Brovoll, Tor Berger,
Tor Sverre Lande, *Fellow, IEEE*, and Svein-Erik Hamran, *Member, IEEE*

Abstract—There has been research interest in using radar for contact-less measurements of the human heartbeat for several years. While many systems have been demonstrated, not much attention have been given to the actual physical causes of why this work. The consensus seems to be that the radar senses small body movements correlated with heartbeats, but whether only the movements of the body surface or reflections from internal organs are also monitored have not been answered definitely. There has recently been proposed another theory that blood perfusion in the skin could be the main reason radars are able to detect heartbeats. In this paper an experimental approach is given to determine the physical causes. The measurement results show that it is the body surface reflections that dominate radar measurements of human heartbeats.

Index Terms—Doppler radar, echocardiography, heart, heart beats, medical radar, non-contact vital signs detection, radar.

I. INTRODUCTION

RADAR can be used to detect a person's heartbeats and respiration contact-less and from a distance, or by placing an antenna on the person's chest or back. Contact-less monitoring of heartbeats and respiration can be useful in long term vital signs monitoring, monitoring elderly people, sleep monitoring or as an early diagnostics tool supplementing already existing technologies. The vital signs are detected by the radar transmitting electromagnetic waves towards the person, and recording the received reflections. When the person is breathing and the heart is beating, modulations occur in the received radar reflections from the person.

Even though it has been a long time since the first radar heartbeat measurements were observed [1], [2], a complete understanding of what is measured has not yet been achieved. The dominating theory on the cause of the observed modulations, is that these are caused by small movements resulting in small phase changes in the received signal. For respiration measurements, the modulation can be seen as an arc in the complex plane compliant with a phase change caused by a moving target [3], [4]. Heartbeat measurements on the other hand, have a more complex shape in the complex plane not immediately recognized as coming from a single moving target.

In [5], the common acceptance that the radar detects heartbeats from small body movements was questioned. They provided a theoretical investigation into various physical mechanisms which could provide an explanation. For far

This work is part of the MELODY project funded by the Research Council of Norway under contract number 187857/S10.

Ø. Aardal, Y. Paichard, S. Brovoll, T. Berger and S-E. Hamran are with Forsvarets forskningsinstitutt (FFI), P.O. Box 25, 2027 Kjeller, Norway e-mail: oyvind.aardal@ffi.no.

S-E. Hamran and T. S. Lande are with the Department of Informatics at the University of Oslo, P.O. Box 1080 Blindern, 0316 Oslo, Norway.

field radar measurements, the following theories on what modulates the received radar signal were presented: Blood perfusion in the skin leading to skin impedance variation, internal body organ movements, skin/body surface movement and variations in black body radiation of the body because of temperature variations. It was concluded that the natural black body radiation cannot be the main cause of the heart signals observed in radar measurements, as the power contribution is too low. Reflections from internal body organs such as the heart walls was discarded as a theory. Simulations show that the reflections from the heart are too small to be of significance, at least when compared to the body surface reflections. This leaves the two theories of blood perfusion and body surface movements.

The calculations in [5] predict that while there could be some contribution in the received radar signals from the body surface movements, the blood perfusion is the main contributor. The beating of the heart leads to cyclic changes in the concentrations of oxygenated blood in human tissues. These changes are also present in the skin and body tissues close to the skin, leading directly to a change in the skin reflection coefficient.

Another issue is whether the heartbeat modulations are solely caused by body surface reflections or if there is a contribution from waves reflected from moving organs within the body such as the heart. It is known that electromagnetic waves can propagate inside the body [5]–[7] and a portion of this wave will be reflected at the boundaries of each tissue back towards the receiving antenna. However, the electric field attenuation in body tissues is high. This coupled with the fact that the air/skin interface provides a strong backscattering suggests that reflections from inside the body does not contribute significantly to the modulations, even though the heart itself has a larger motion than the chest surface. This has been assessed through simulations [6]–[8], but to the authors' knowledge has not yet been confirmed experimentally.

Fig. 1 shows a typical remote heartbeat monitoring setup. The main objective of this paper is to present an experimental approach to address the following questions:

- Are the observed radar modulations caused by body movements or blood perfusion in the skin?
- Is there sufficient penetration of electromagnetic (EM) waves inside the body so that the actual movement of the heart is seen in non-contact radar measurements?

The experimental approach to answering these questions was based on some simple principles: If the modulations are caused by the chest displacement of the person, reducing the movement will also reduce the observed modulations. If the modulations are caused by changes in skin properties, concealing the skin from the radar waves will reduce the

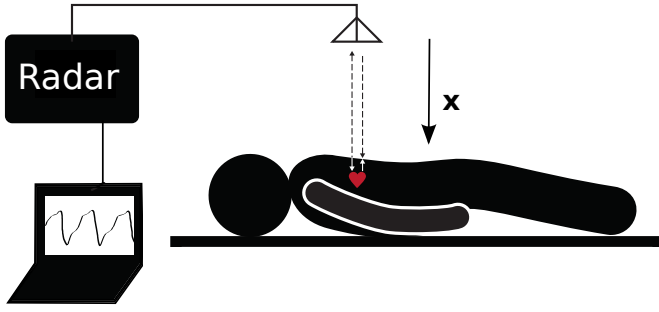


Fig. 1. A typical non-contact radar heartbeat measurement. An antenna is aiming at a person's chest, and regular modulations correlated with the person's heartbeats are observed.

observed modulations. Reversely, hindering the movement will not have an effect on the modulations if they are caused by skin property changes. Likewise, concealing the skin without hindering movement will not have an effect on the modulations if they are caused by chest movement.

Based on the mentioned principles, the following experiment was designed. Measurements of a person's heartbeat were conducted normally to be used as a reference. Then, the person's chest was pressed flat by a transparent plexiglass plate, hindering the movement of the chest. Third, the person's chest was covered in a thin film of silver concealing the radar waves from being reflected from the skin while not hindering the movement.

Before the experiments are described, theoretical background on electromagnetic waves interacting with the human body is given in the next section. Here, two main theories of blood perfusion versus chest movement are also discussed. In Section III the experimental setups and data analysis methods are described. Last, the results are presented in sections IV and V.

II. ELECTROMAGNETIC WAVE INTERACTION WITH THE HUMAN BODY

An electromagnetic wave travelling through a medium with permittivity ϵ' , conductivity σ and magnetic permeability μ will at position x and time t have an electric field:

$$E(x, t) = \mathbf{Re}\{E_0 e^{-\alpha x - ikx + i\omega t}\} \quad (1)$$

$$\alpha = \omega \sqrt{\mu \epsilon'} \left\{ \frac{1}{2} \left[\sqrt{1 + \left(\frac{\sigma}{\omega \epsilon'} \right)^2} - 1 \right] \right\}^{1/2} \quad (2)$$

$$k = \frac{\omega}{v} = \omega \sqrt{\mu \epsilon'} \left\{ \frac{1}{2} \left[\sqrt{1 + \left(\frac{\sigma}{\omega \epsilon'} \right)^2} + 1 \right] \right\}^{1/2} \quad (3)$$

where ω is the angular frequency, E_0 is the initial value of the electric field, v is the speed of propagation in the medium, α the attenuation constant of the medium and k the phase constant. For air and body tissues the magnetic permeability is equal to the free space permeability $\mu = \mu_0$.

An electromagnetic wave transmitted a sufficient distance from a human body will hit the body as a plane wave. Here, two factors determine the scattering of the wave: The shape of the body and the body dielectric properties. The shape of the body varies from person to person and with posture, while

the dielectric properties are similar. For this reason, the shape of the body is disregarded in the following theory. Thus the theory is not accurate for a real world scenario, but sets the orders of magnitude for the reflection and attenuation of the EM waves. This illustrates the scattering from the body surface and the attenuation of the wave travelling inside the body.

When the wave hits an interface between two media with different dielectric properties, part of the wave is reflected while part of the wave is transmitted into the second medium. For normal incident waves on a planar surface, the reflected and transmitted electric fields are given by

$$E_r(x, t) = \mathbf{Re}\{\Gamma E_0 e^{\alpha_1 x + ik_1 x + i\omega t}\} \quad (4)$$

$$E_t(x, t) = \mathbf{Re}\{T E_0 e^{-\alpha_2 x - ik_2 x + i\omega t}\}. \quad (5)$$

Note that the scattered wave $E_r(x, t)$ is travelling in the negative x direction, while the transmitted wave $E_t(x, t)$ is travelling in the positive direction. The reflection coefficient Γ and transmission coefficient T between medium 1 and 2 are connected to the dielectric constants by

$$\Gamma_{1/2} = \frac{\eta_2 - \eta_1}{\eta_2 + \eta_1} \quad (6)$$

$$T_{1/2} = \frac{2\eta_2}{\eta_2 + \eta_1}, \quad (7)$$

where

$$\eta_n = \sqrt{\frac{i\omega\mu}{\sigma_n + i\omega\epsilon'_n}}. \quad (8)$$

Using the Gabriel & Gabriel database for dielectric properties of human tissues [9]–[11] the air to skin reflection coefficient $\Gamma_{air/skin}$ can be found as a function of frequency, the results seen in Fig. 2. This agrees with the results by [12] where the reflection between air and skin was calculated to be 72.7% at 1.4 GHz.

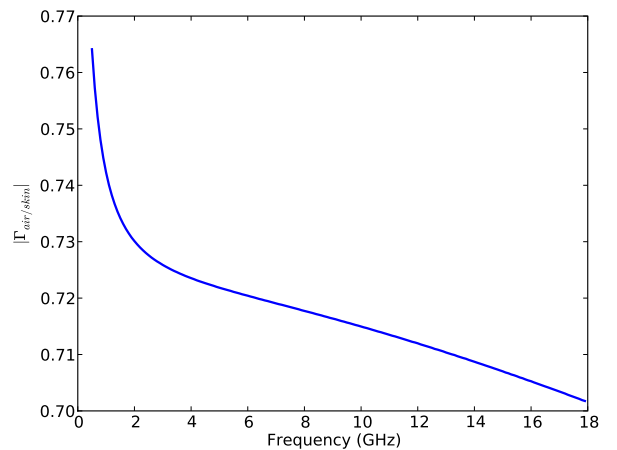


Fig. 2. The magnitude of the reflection coefficient $|\Gamma_{air/skin}|$ between air and skin as a function of frequency.

The tissue parameters ϵ' and σ vary with frequency. For all tissues between the skin and the heart wall (skin, fat, muscle, bone, blood) the conductivity is increasing with frequency, which through (2) increases the attenuation with frequency.

Several simulation studies have been performed on the attenuation of electromagnetic waves in the human body, confirming these results. Simulations by [6] show a two way attenuation of a 1.5 GHz wave between the chest and heart to be 40 dB. In [7] the total loss on the two way travel distance was reported to be about 60 dB at 3 GHz, rising to about 160 dB at 10 GHz with an average power loss of 80 dB in the band. A circuit model by [8] provides attenuation of about 25 dB at 100 MHz increasing to about 50-55 dB at 3 GHz.

A large part of the incoming wave at the air/skin interface is scattered, while there is great attenuation of the wave traveling inside the human body according to the results mentioned above. Even though the radar receiver may pick up some signal from inside the body, the body surface scattering is much stronger and with a similar periodic movement, making it unrealistic to separate the in-body response from the strong surface response. This leads to the conclusion, from theory, that the body surface scattering dominate ranged measurements. This theory is further strengthened by the experimental results presented later in this paper.

Radar recordings using I & Q sampling can be displayed in the complex plane [3]. An actual radar recorded heartbeat is displayed in Fig. 3 and Fig. 4. The displayed data is a single frequency continuous wave (CW) recording of several heartbeats that have been high-pass filtered to remove stationary components and slow movements. The modulation follows a

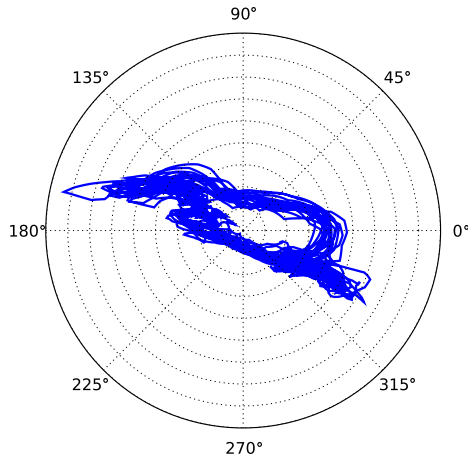


Fig. 3. A 2 GHz CW recording of several heartbeats seen in the complex plane. The axes are linear scale with the real part of the voltage along the horizontal axis and the imaginary part of the voltage along the vertical axis. The mean has been subtracted from the data.

complex shape in the complex plane, and is not a pure phase or amplitude modulation.

There are, theoretically, more than one way the observed radar modulations can be created. The most common theory in the literature on the heartbeat modulation seen in radar recordings is that it stems from body movements caused by the heartbeat. The beating heart causes millimeter to sub-millimeter movements on the chest surface. Throbbing blood veins and changes in the body's gravitational center with the heartbeat are also body movements closely connected to the heartbeat. Movements on this small scale are recorded as phase

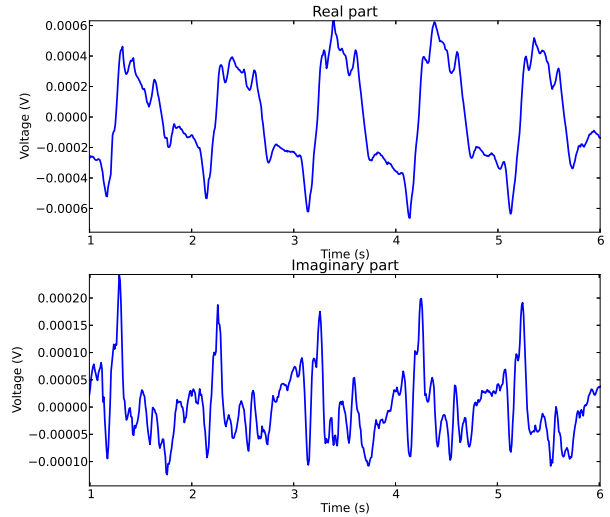


Fig. 4. The real and imaginary part of an example non-contact recording of heartbeats using 2 GHz CW radar.

changes by the radar receiver.

As mentioned in the introduction, the other most plausible theory on what we see when observing heartbeats with radar is that we are seeing changes in the electromagnetic properties of the skin. This theory, called the blood perfusion theory, is explored in the following section. Attention is then turned to the body movement theory.

A. Blood perfusion theory

During a heartbeat, the density of blood in the skin changes slightly [5]. The skin reflection coefficient changes accordingly; with no change in blood density in the skin, there will be no reflection coefficient changes. If on the other hand the blood density changes from 0 % to 100% , the reflection coefficient would change from the skin reflection coefficient $\Gamma_{air/skin}$ to the blood reflection coefficient $\Gamma_{air/blood}$. During a heartbeat the blood density change will be much less than 100%, meaning that the change in reflection coefficient during a heartbeat will be much less than the difference between $\Gamma_{air/skin}$ and $\Gamma_{air/blood}$. For the sake of analysis though, one can look at the extreme cases of a pure air/skin interface and a pure air/blood interface. These reflection coefficients can be computed using Gabriel et. al.'s database [9]–[11] and equations (6) and (8). The difference in reflection coefficient between these two cases, $\Delta\Gamma = |\Gamma_{air/skin} - \Gamma_{air/blood}|$, is plotted in Fig. 5.

The reflection coefficient is connected to the radar cross section of a target through

$$RCS_P = W\Gamma^2, \quad (9)$$

where RCS_P is the radar cross section of the person and W is the radar cross section of the person if he had been perfectly conductive.

Assuming that what is seen in a radar heartbeat recording is the blood perfusion, this will be seen as a change in the

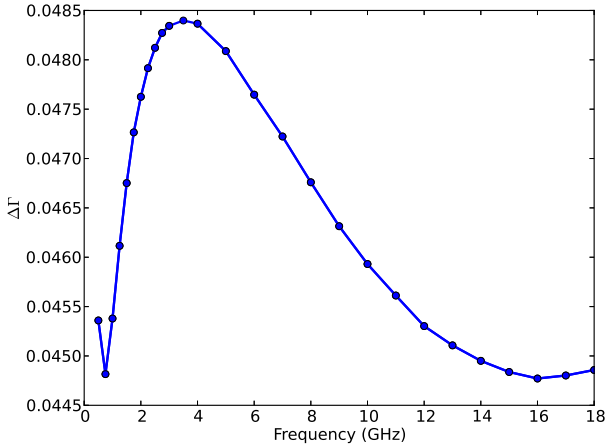


Fig. 5. Difference in reflection coefficient $\Delta\Gamma$ between an air/skin interface ($\Gamma_{air/skin}$) and an air/blood interface ($\Gamma_{air/blood}$).

RCS through the relation

$$\Delta RCS_P = W\Delta\Gamma^2, \quad (10)$$

where $\Delta\Gamma$ is the actual change in skin reflection coefficient of the person. Any contribution to the observed modulation from the blood perfusion effect will manifest itself as amplitude modulations in the person echo. These are modulations that would be present regardless of any movements of the person. Since the chest of a person spans a small range of distances from the radar, the amplitude modulations may appear at slightly different ranges. Such a scenario is compliant with the modulation seen in Fig. 3

B. Body movement theory

In the body movement theory, the observed radar modulation is explained as small chest movements causing phase variations in the received signal. A single point scatterer with a time varying distance from the antennas will be seen as a pure phase change directly proportional to the movement. In baseband, this can be written $Ae^{\phi(t)}$, where A is the amplitude of the signal and $\phi(t) = \frac{2\omega R(t)}{c}$ is the time varying phase. ω is the signal angular frequency, $R(t)$ is the time varying range and c is the speed of light. The amplitude of the signal is dependent on the object's RCS.

The human chest however, is not a point scatterer. Different parts of the chest are at slightly different distances R from the radar antenna. The total contribution from the moving parts of the chest is a sum of the reflections over all the ranges R :

$$A_m(t)e^{i\phi_m(t)} = \int_{R_0}^{R_1} A_m(R)e^{i\phi_m(R,t)} dR, \quad (11)$$

$$\phi_m(R,t) = \frac{2\omega R(t)}{c}, \quad (12)$$

with R_0 being the range to the closest part of the moving chest, and R_1 the range to the farthest part of the moving chest. From the equation, the resulting vector has modulations both in amplitude and phase because phase modulations from

different ranges have been summed. Contributions from the static scatterers such as the non-moving parts of the body are also part of the received signal. The sum of these contributions will have non-varying amplitude and phase, $A_s e^{i\phi_s}$. The total received signal is the sum of the static and moving parts:

$$b(t) = A_s e^{i\phi_s} + A_m(t) e^{i\phi_m(t)}. \quad (13)$$

This theory is also compliant with the observed heartbeats plotted in Fig. 3. For more details on the complex modulation of heartbeat recordings and the movement theory, the reader is referred to [13] and [3].

III. MEASUREMENTS AND METHODOLOGY

As explained, the recorded heartbeat modulations are complex in shape and fits both the blood perfusion model and the body movement model. In this section, our experimental approach to finding the correct explanation for the modulations is described. The experiment consists of three measurement setups and post processing. The first setup, called the bare measurement, is of a person lying on his back with a bare chest and the radar antenna above the chest. The second setup, called the plexiglass measurement, is the same setup with the person's chest being pressed flat by a plexiglass plate. Last is the silver measurement, where the person's chest is covered in a layer of silver leaves.

A. The experimental setup

All measurements were conducted on a male subject of age 26 in an anechoic chamber using a vector network analyzer [14]. A network analyzer transmits electromagnetic signals and measures the phase and amplitudes of the reflections. With antennas connected to the network analyzer, it can be used as a radar. The transmitted signals were single frequency continuous waves with an IF bandwidth of 100 Hz which were sampled at 113 Hz sampling frequency. Two different antennas were used, one for the 0.5-4 GHz range and one for the 4-18 GHz range. Fig. 6 shows the measurement setup.

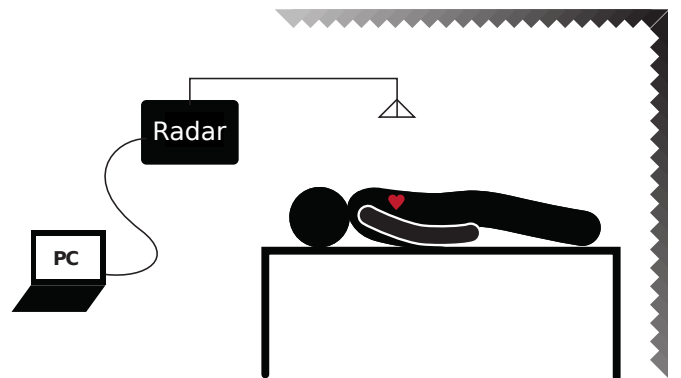


Fig. 6. The measurement setup. The person was lying on a table placed inside an anechoic chamber. An antenna was placed over the person directed towards his chest, and connected with the network analyzer placed outside of the anechoic chamber.

A series of 155 measurements using three different setups has been performed. The measurements were performed using

0.6, 1, 2, 3, 4, 8, 12, 15 and 18 GHz Tx frequencies. In the first setup, seen in Fig. 7, a person is lying on his back with an antenna directly above aimed down at the chest. In Fig. 8, the

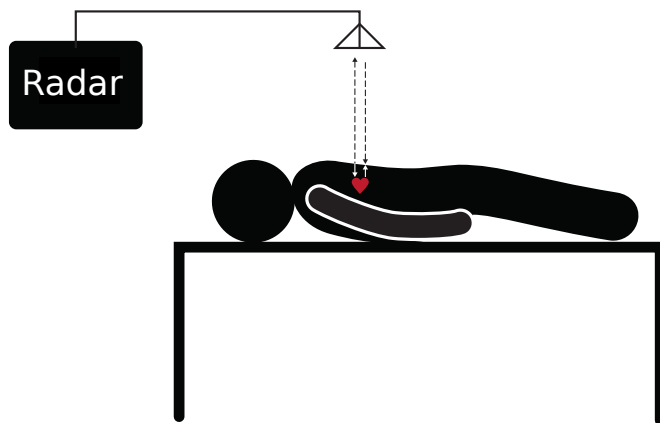


Fig. 7. The test person with a bare chest.

plexiglass setup where the test person's chest is pressed flat by a plexiglass plate is shown. This suppresses any modulation caused by movement in the radar recordings because the chest is hindered from moving by the plexiglass plate. Modulation caused by blood perfusion on the other hand should stay the same or be magnified because the gain of the chest is increased when pressed flat. In addition, any modulation caused by

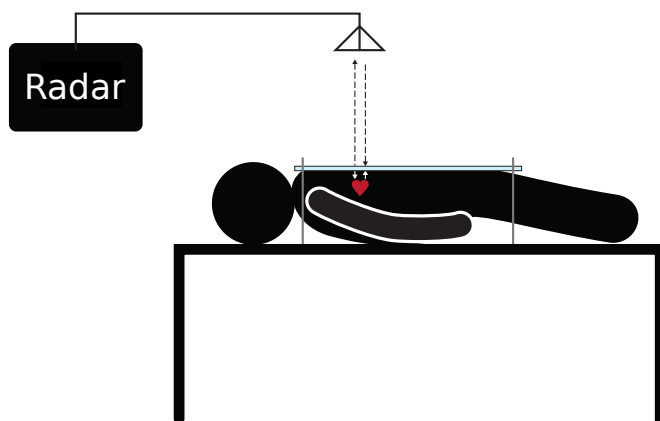


Fig. 8. The test person with a plexiglass pressing tightly against his chest. Note that most of the person's chest directly under the antenna is now pressed flat and is prevented from moving by the stiff plexiglass plate. The sides of the torso, as well as the area by the neck though are still free to move.

reflections from moving internal body parts such as the heart should not be much affected. Waves penetrating into the chest and being reflected from the moving heart should not be suppressed compared to the bare chest measurements. From modelling however, this is not expected to be noticeable as the attenuation is too large.

The third measurement setup, showed in Fig. 9, is of the test person with his chest covered in silver leaves. The silver leaves are squares of thin silver film, which stick to the skin and follow the contours of the body closely. Silver is a conducting material, which blocks electromagnetic waves from penetrating into the body tissues and will reflect any

incoming fields back. In this scenario, the radar modulation caused by movement should stay the same or be magnified because of the increased reflection. The chest surface reflection coefficient is increased from $|\Gamma| \approx 0.7$ to $|\Gamma| \approx 1$ when the silver leaves are applied, increasing the reflected power because of the increased conductivity in (6). On the other hand, the modulation caused by blood perfusion should be greatly decreased, as the largest contributor to this modulation is covered in metal. Additionally, no penetration of the EM

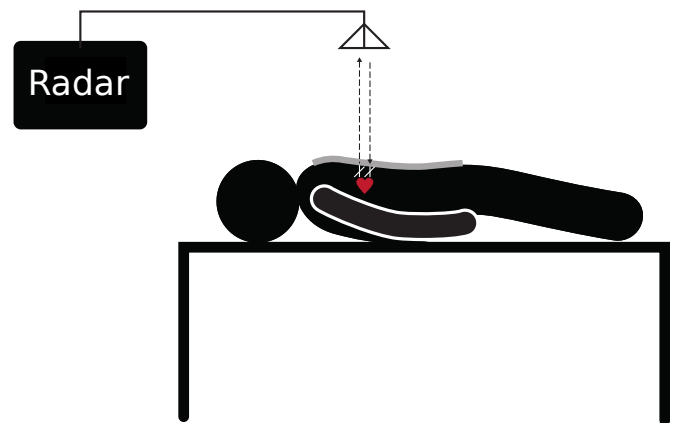


Fig. 9. The test person's chest and stomach has been covered with a thin layer of silver leaves. Since the area of the person within the antenna main lobe is covered, the majority of the reflections from the person back to the antenna is from this region.

waves into the person's torso will occur. Thus only surface motion modulation from the chest and other body parts can occur in the radar recording. All these measurements were conducted with the person lying in the same spot, making the only change between the measurements being whether the chest was bare or covered with plexiglass or silver leaves.

B. Processing

The bare, plexiglass and silver measurements need some processing of the data before results can be extracted. The aim of the experiments is to compare the sizes of the modulation using the three explained measurement setups. Therefore, it is important for the processing to provide a robust and simple measure of the modulation size without introducing any unnecessary error sources. With this in mind, the post processing of the data is explained here.

As Fig. 3 shows, the actual modulation follows a complex shape that varies between persons, aspect angle and frequency. However, the modulation occurs along one main direction. When considering the blood perfusion model, this main direction of modulation is the change in RCS. In the movement model this main direction is connected to the phase change from the changing range to the chest. In both cases though, it is the main direction of modulation that will be used in this investigation.

To compare the modulation in different measurements, we used a procedure to rotate the modulation to always lie along the real axis, similar to the linear regression method presented in [15]. First, the mean is subtracted from the data to center it

around the origin. Then, a linear least squares fit of a straight line to the data set is made in the complex plane. The angle this straight line approximation has to the real axis is subtracted from the data vector, resulting in the data vector having its main direction of modulation along the real axis. Keeping the real part and discarding the imaginary part, leaves only the main modulation in the measurement vector.

The filtering and rotation of the measurement explained in the last paragraph leaves a vector \tilde{b} of real values containing the modulation along the main modulation axis. A measure of the size of the heartbeat modulation through several heartbeats is to take the mean absolute value of this vector:

$$\hat{M} = \sum_{n=0}^{N-1} \frac{|\tilde{b}_n|}{N}, \quad (14)$$

where N is the length of the modulation vector \tilde{b} . Several measurements were conducted for each frequency and setup, and the mean value of the modulations \hat{M} for each frequency is denoted \tilde{M} .

The goal of the experiments is to find out if the modulation is bigger or smaller when applying the plexiglass or silver leaves to the chest compared to the bare chest modulation. This goal is achieved by computing the ratios:

$$\text{plexi/bare ratio} = \frac{\tilde{M}_{plexi}}{\tilde{M}_{bare}} \quad (15)$$

$$\text{silver/bare ratio} = \frac{\tilde{M}_{silver}}{\tilde{M}_{bare}}. \quad (16)$$

A ratio of one means that the modulation is the same size as in the reference bare chest modulation. A ratio less than one means that the modulation is less, while a ratio greater than one means that the modulation has increased compared to the bare chest modulation.

In addition to comparing the magnitudes of the modulations, the heartbeat waveforms recorded using the three experimental setups were compared. From each measurement \tilde{b} , a series of ten heartbeats were picked out, each series starting at the same phase of the heartbeat. Each series were re-sampled to be of the same number of samples in total. For each experimental setup, several measurements were performed at each frequency. The mean measurement series were made, such that each of the bare chest, silver and plexiglass setups has one mean measurement \tilde{b} ten heartbeats long for each tested frequency. These mean measurements were used to compare the shape of the silver and plexiglass waveforms to the bare chest waveforms through the normalized cross correlation:

$$\rho = \frac{\sum_{n=1}^N \tilde{b}_{1,n} \tilde{b}_{2,n}}{N \sigma_1 \sigma_2}, \quad (17)$$

where ρ is the normalized cross correlation with zero delay, N is the number of samples in each time series, σ_1 is the standard deviation of \tilde{b}_1 and σ_2 is the standard deviation of \tilde{b}_2 . The bare chest waveforms were used as \tilde{b}_2 , while either the silver or the plexiglass waveforms were used as \tilde{b}_1 .

IV. RESULTS

A total of 155 measurements were conducted, distributed as plexiglass, silver leaf and bare chest measurements. The measurements were conducted at 0.6, 1, 2, 3, 4, 8, 12, 15 and 18 GHz Tx frequency.

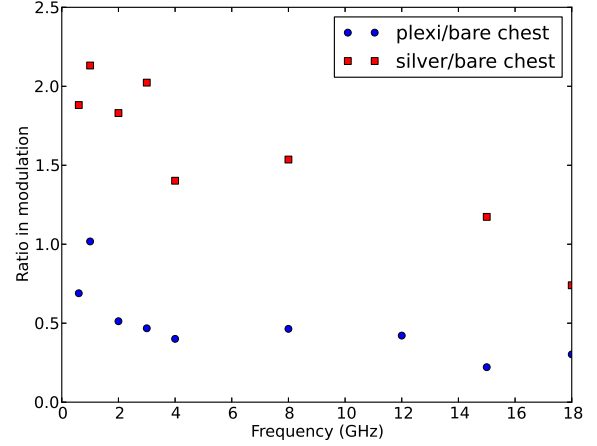


Fig. 10. The ratio between the modulation in plexiglass covered chest and bare chest and between silver covered chest and bare chest. For most frequencies, the modulation is smaller with the plexiglass covered chest while it is larger for silver covered chest.

For all the tested frequencies, the data were processed as outlined in Section III-B. Using (14), a measure \tilde{M} of the modulation was found for each of the three measurement setups for each frequency. The ratios (15) and (16) were computed for each frequency, and plotted in Fig. 10. It is seen that the modulation was reduced when the plexiglass plate was pressing the chest flat. Had the main contributor to the modulation been blood perfusion or reflections from internal organs, this reduction in modulation would not have been observed. The RCS of the chest remained approximately the same, but the phase modulation from movement was reduced. It is noted however that the modulation was not completely suppressed. For the lower frequencies this could in part be from waves penetrating the chest and reflecting of the heart wall, although this is unlikely. Parts of the body that were not hindered from moving by the plexiglass plate could be a contributor to the modulation. However, while the plexiglass plate suppressed chest movements, it did not completely remove them.

When the chest was covered in silver leaves, the modulation was larger than when the chest was bare. This dispels the blood perfusion theory, as the modulation increased when most of the skin in the antenna main beam was concealed. An example time series from each of the three setups recorded at 15 GHz has been plotted on top of each other in Fig. 11. For each frequency, the silver and plexiglass waveforms were compared to the bare chest waveform through the normalized cross correlation. The results are plotted in Figure 12. With the exception of the 4 GHz measurements, the silver leaf recordings show good correlation with the bare chest recordings. The plexiglass measurements show good correlation at frequencies below 2

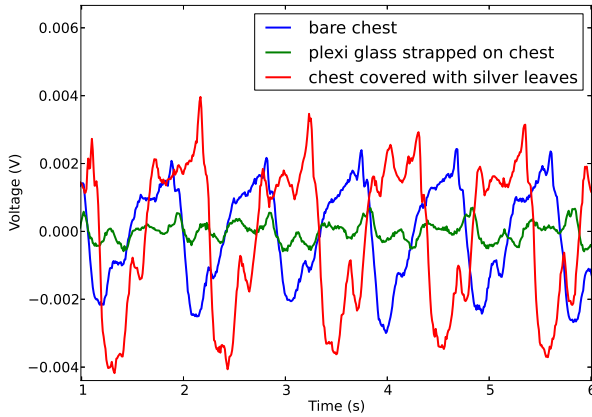


Fig. 11. The heartbeats measured on a bare chest, a chest covered in silver leaves and the chest under pressure from a plexiglass plate. All measurements were conducted under the same conditions, with the only change being the chest covered in silver, plexiglass or being bare. Note that the plexiglass measurement modulation is decreased while the silver leaves measurement modulation is increased compared to the bare chest measurement.

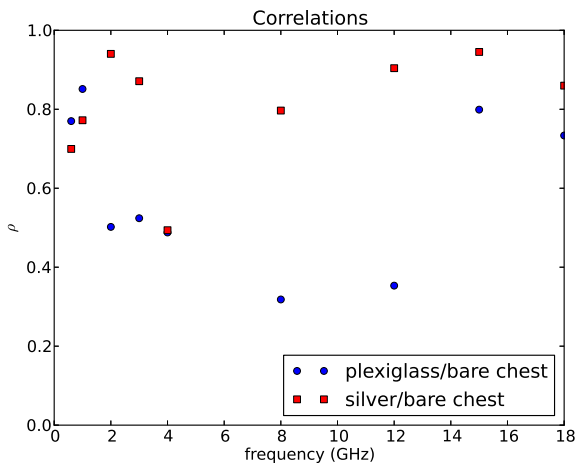


Fig. 12. The normalized cross correlation ρ between plexiglass and bare chest measurements and between silver and bare chest measurements as a function of frequency.

GHz but worse at higher frequencies. At the lower frequencies the changes in chest morphology are small compared to the wavelength, and the waveform is not expected to change much in shape from the plexiglass pressing down on the chest. The heartbeat waveform is similar in shape but increased in magnitude when the chest is covered in silver leaves, which supports the theory of the modulations being caused by body surface reflections. In this case, the phase modulations from the movements stayed similar, while the RCS was increased from the silver leaves.

To be sure that the plexiglass plate was actually suppressing the movement of the chest, an accelerometer was placed on the chest in some of the bare chest measurements, and on the same location on the plexiglass plate in some of the plexiglass measurements. On average the movement of the chest with the plexiglass tightened was one third that of the

bare chest, confirming that the chest surface movement was indeed decreased during the plexiglass measurements.

V. DISCUSSION

The bare, silver and plexiglass measurements dispels the theory that changes in blood density in the skin are the cause of modulations seen in radar recordings, while confirming the theory that the chest movement caused by the heartbeat is seen. For all tested frequencies except 18 GHz the modulation was larger with the chest covered in silver leaves than with a bare chest or the chest pressed flat with the plexiglass plate. While this indicates that the chest movement dominates the modulation, the modulation in the 1 GHz plexiglass measurements are on average about as large as the modulation in the bare chest measurements. Using an accelerometer it was established that the chest movement was reduced as much in the 1 GHz plexiglass measurements as for the other frequencies, so other explanations need to be sought for this particular result. One explanation is possible penetration of the EM wave into the chest, meaning the modulation is from reflections from the actual heart movement. However, there is significant attenuation in the body tissues at this frequency, meaning that it is unlikely that the modulation would be as big as the modulation caused by surface movements. Another explanation is that it is movements from other parts of the body than the chest area under the plexiglass plate that is seen. The upper part and sides of the torso are unaffected by the plexiglass plate. At the lower frequencies, the used antenna is much less directional than at the higher frequencies. Thus, not only the chest is present in the antenna main beam, and the rest of the body will contribute more in the receiver. Indeed, in [16] it was found that respiration can be detected using radar by only looking at the arm of a person.

Movements of other parts of the body than the chest could have a significant effect on the modulation seen in the radar receiver. Penetration into the body at sub-GHz frequencies cannot be totally ruled out, and movements from other body parts stand as a plausible significant contributor to the total modulation. When looking at the results in total though, the bare, plexiglass, silver measurements show that the dominant cause of the heartbeat modulations is the chest surface movement.

A large portion of the research on remote heartbeat detection using radar have focused on Ultra wideband (UWB), with one of the reasons being the good penetration of the lower frequencies. From the results in this paper, the heartbeat modulations are dominated by chest surface movements. Higher frequencies are better suited for detection of small movements, as the movements will increase relative to the wavelength with higher frequencies. Narrow band radars operating at high microwave or even millimeter-wave frequencies will thus be better suited for remote heartbeat detection than low frequency or UWB systems. This is however, only valid for remote detection as antennas placed in contact with the chest are not dominated by the chest surface reflection and may receive reflections from the actual heart.

VI. CONCLUSION

An experimental approach was taken to answer the question of what is actually measured in a non-contact radar heartbeat measurement. The three tested theories were blood perfusion in the skin, body surface movements and internal body organ movements. To test the hypotheses, three measurement setups of a person under normal conditions, with chest movement constrained and with skin tissue properties concealed were performed over the 0.5 – 18 GHz frequency range. The chest movement was constrained by pressing the chest of the person under test flat using a plexiglass plate. To conceal the skin tissue properties without affecting the movements the chest was covered in thin silver leaves. The results show that it is body surface movements that are dominating remote radar measurements of heartbeats.

REFERENCES

- [1] C. Johnson and A. Guy, "Nonionizing electromagnetic wave effects in biological materials and systems," *Proceedings of the IEEE*, vol. 60, no. 6, pp. 692–718, June 1972.
- [2] J. Lin, J. Kiernicki, M. Kiernicki, and P. Wollschlaeger, "Microwave apexcardiography," *Microwave Theory and Techniques, IEEE Transactions on*, vol. 27, no. 6, pp. 618–620, Jun 1979.
- [3] Ø. Aardal, S.-E. Hamran, T. Berger, Y. Paichard, and T. S. Lande, "Chest movement estimation from radar modulation caused by heartbeats," in *Biomedical circuits and systems conference (BIOCAS 2011), 2011 IEEE*, November, pp. 452–455.
- [4] B.-K. Park, O. Boric-Lubecke, and V. M. Lubecke, "Arctangent Demodulation With DC Offset Compensation in Quadrature Doppler Radar Receiver Systems," *Microwave Theory and Techniques, IEEE Transactions on*, vol. 55, no. 5, pp. 1073–1079, May 2007.
- [5] G. Varotto and E. Staderini, "On the UWB medical radars working principles," *International Journal of Ultra Wideband Communications and Systems*, vol. 2, no. 2, pp. 83–93, 2011.
- [6] E. Staderini, "UWB radars in medicine," *Aerospace and Electronic Systems Magazine, IEEE*, vol. 17, no. 1, pp. 13–18, Jan 2002.
- [7] D. Zito, D. Pepe, B. Neri, D. De Rossi, A. Lanata, A. Tognetti, and E. Scilingo, "Wearable System-on-a-Chip UWB Radar for Health Care and its Application to the Safety Improvement of Emergency Operators," in *Engineering in Medicine and Biology Society, 2007. EMBS 2007. 29th Annual International Conference of the IEEE*, Aug. 2007, pp. 2651 – 2654.
- [8] S. Pisa, P. Bernardi, M. Cavagnaro, E. Pittella, and E. Piuze, "Monitoring of cardio-pulmonary activity with UWB radar: A circuitual model," in *Electromagnetic Compatibility and 19th International Zurich Symposium on Electromagnetic Compatibility, 2008. APEMC 2008. Asia-Pacific Symposium on*, May 2008, pp. 224–227.
- [9] C. Gabriel, S. Gabriel, and E. Corthout, "The dielectric properties of biological tissues: I. Literature survey," *Physics in medicine and biology*, vol. 41, p. 2231, november 1996.
- [10] S. Gabriel, R. Lau, and C. Gabriel, "The dielectric properties of biological tissues: II. Measurements in the frequency range 10 Hz to 20 GHz," *Physics in medicine and biology*, vol. 41, p. 2251, november 1996.
- [11] —, "The dielectric properties of biological tissues: III. Parametric models for the dielectric spectrum of tissues," *Physics in medicine and biology*, vol. 41, p. 2271, november 1996.
- [12] G. Ossberger, T. Buchegger, E. Schimback, A. Stelzer, and R. Weigel, "Non-invasive respiratory movement detection and monitoring of hidden humans using ultra wideband pulse radar," *Ultra Wideband Systems, 2004. Joint with Conference on Ultrawideband Systems and Technologies. Joint UWBST & IWUWBS. 2004 International Workshop on*, pp. 395–399, May 2004.
- [13] C. Li and J. Lin, "Random Body Movement Cancellation in Doppler Radar Vital Sign Detection," *Microwave Theory and Techniques, IEEE Transactions on*, vol. 56, no. 12, pp. 3143–3152, dec. 2008.
- [14] "Agilent Network Analyzer N5245A PNA-X, <http://www.home.agilent.com/agilent/product.jsp?nid=536902643.898624.00&cc=NO&lc=eng>."
- [15] D. R. Morgan and M. G. Zierdt, "Novel signal processing techniques for doppler radar cardiopulmonary sensing," *Signal Process.*, vol. 89, no. 1, pp. 45–66, 2009.
- [16] K. Mostov, E. Liptsen, and R. Boutchko, "Medical applications of shortwave FM radar: Remote monitoring of cardiac and respiratory motion," *Medical physics*, vol. 37, p. 1332, 2010.



radar.

Øyvind Aardal Øyvind Aardal was born in Skedsmo, Norway, in 1984. He received the B.Sc. degree and the M.Sc. degree in applied mathematics from the University of Oslo, Norway, in 2006 and 2008 respectively.

In the summer of 2007 he was a lecturer in mathematics at Oslo University College. Since 2009 he has been with the Norwegian Defense Research Establishment (FFI), Kjeller, Norway, where he is currently working towards his Ph.D. His research interests include radar signal processing and medical



applied to micro-Doppler measurements. In 2008, he joined the Radar Remote Sensing Group at the University of Cape Town (UCT) as a lecturer, where he was involved in the design of passive coherent location radars and multistatic radars. Since 2010 he has been with the Norwegian Defense Research Establishment, where he is doing research on remote sensing of vital signs using radar techniques. His research interests include the design of radars, antennas and microwave systems.

Yoann Paichard Yoann Paichard (M'05) received the M.Eng. degree in Electrical Engineering from the National Institute of Applied Science, Rennes (France) in 2001, the M.Sc. degree in Electronics and Communications Systems from the University of Pierre & Marie Curie, Paris in 2003 and the Ph.D. degree in Physics from the University of Paris-Sud in 2007.

From 2003 to 2007, he carried out research at the French Aerospace Lab (ONERA, France) on ultra-wideband radars and on real-time imaging radars



Sverre Brovoll Sverre Brovoll was born in Arendal, Norway, in 1979. He received the M.Sc degree in cybernetics from the Norwegian University of Science and Technology, Trondheim, in 2006.

In 2006 he started working with synthetic aperture radar systems as a scientist at FFI. In 2011 he began his work toward a Ph.D. degree in the field of medical radar systems at FFI and the department of informatics at the University of Oslo



Tor Berger Tor Berger received the M.Sc. degree and the Dr. Scient degree in applied physics from the University of Tromsø, Norway, in 1992 and 1996, respectively.

Since 1996 he has been with His main field of work is within radar signal processing, focusing on motion compensation techniques and synthetic aperture radar imaging.



Tor Sverre Lande Tor Sverre Lande is a professor in the Microelectronic/nanoelectronics at Dept. of Informatics, Univ. of Oslo as well as visiting professor at Institute of Biomedical Engineering, Imperial College, London, UK. His primary research is related to microelectronics, both digital and analog. Research fields are Neuromorphic Engineering, analog signal processing, subthreshold circuit and system design, biomedical circuits and systems and impulse radio (UWB). Research efforts on impulse radar using continuous-time binary value coding (CTBV) is now commercialized as a spin-off company, Novelda AS (www.novelda.no). He is the author or co-author of more than 120 scientific publications with chapters in two books. He is currently serving as an associate editor of several scientific journals. He has served as guest editor of special issues like IEEE Transactions on Circuits and Systems, vol II and IEEE Transactions on Circuits and Systems, vol I, special issue on "Biomedical Circuits and Systems". He is/has been a technical committee member of several international conferences and has served as reviewer for a number of international technical journals. He has served as Technical Program Chair for several international conferences (ISCAS 2003 in Bangkok, NORCHIP 2004 in Oslo, BioCAS workshop 2004 in Singapore, BioCAS 2006 in UK, BioCAS2010, ISCAS 2011). He was chair elect (2003-2005) of the IEEE Biomedical Circuits and Systems technical committee (BioCAS) and is also a member of other CAS technical committee. In 2006 he was appointed Distinguished Lecturer of the IEEE Circuits and Systems Society (CAS) and elected member of CAS Board of Governors. He is currently serving as Vice-President of Conferences in the CAS Society. He is also the founding Editor-in-Chief of IEEE Transactions on Biomedical Circuits and Systems (2007-2010s). In 2010 appointed Fellow of the IEEE.



Svein-Erik Hamran Svein-Erik Hamran received an MSc in Technical Physics in 1984 from the Norwegian Institute of Technology (NTNU, Trondheim, Norway) and a Dr Scient degree in 1990 in Applied Physics from the University of Tromsø. He worked from 1985 to 1996 at the Environmental Surveillance Technology Programme and was in 1989/90 a Visiting Scientist at CNRS Service d'Aéronomie, Paris, France. From 1996 he has been at the Norwegian Defense Research Establishment working as a Chief Scientist managing radar programs. From 2001 to 2011 he was an Adjunct Professor in Environmental Geophysics at the Department of Geosciences, University of Oslo. From 2011 he is an adjunct professor at the Department of Informatics at the University of Oslo. He is a co-investigator on the ESA satellite ROSETTA experiment Comet Nucleus Sounding Experiment by Radiowave Transmission, CONCERT and a Co-Principal Investigator on the WISDOM GPR experiment on the ESA ExoMars satellite. His main interest is UWB radar design, radar imaging and modelling in medical and ground penetrating radar.